BEYOND CANLUB: AN IMPROVED ALTERNATIVE COATING DEVELOPMENT

M. Farahani, G.A. Ferrier, P.K. Chan*, and E.C. Corcoran[†]
Department of Chemistry and Chemical Engineering, Royal Military College of Canada
P.O. Box 17000, Kingston, ON, Canada K7K-7B4
(* Phone: (613) 541-6000 ext. 6145; E-mail: Paul.Chan@rmc.ca)

(†Phone: (613) 541-6000 ext. 3508; E-mail: Emily.Corcoran@rmc.ca)

A. Pant

Cameco Fuel Manufacturing Limited, Port Hope/Cobourg, Ontario, Canada

ABSTRACT – The CANLUB graphite coating is exclusively used in CANDU nuclear reactors to protect fuel sheaths from stress corrosion cracking. However, uncertainties regarding its quality control, manufacturing continuity, and performance at high burnups provide sufficient motivation for exploring alternative coating materials. Since the chemistry of polysiloxanes may offer improved protection against stress corrosion cracking, we describe the physical and elemental characterization of CANLUB and three commercial polysiloxane coatings. Preliminary results suggest that the Pyromark coating has the greatest potential to replace the CANLUB coating.

1. Introduction

The CANLUB coating effectively mitigates CANDU fuel failures due to stress corrosion cracking (SCC) (failure rate ~ 0.01%). However, Canadian fuel manufacturers (CFM¹ and GEH-C²) are concerned about the supply of CANLUB material because of the limited number of qualified suppliers. These concerns are shared by the Canadian nuclear industry. The reduced performance of CANLUB at high burnups makes CANLUB a limiting factor when implementing advanced fuel cycles [1]. Furthermore, CANLUB is potentially vulnerable to having a single SCC mitigation process [2], which is sensitive to the chemical makeup of CANLUB. Consequently, alternative coatings that are chemically robust, readily available, and compatible with existing fuel manufacturing processes are being investigated.

Although various CANLUB coatings have already been investigated (DAG-154, ES-242, and siloxane), the DAG-154 remains the only protective coating used in CANDU® reactors. The development of alternative coatings has been generally slow, quite possibly because the above coatings behaved similarly in providing protection against SCC [3]. Vacuum grease, a siloxane coating, demonstrated good performance against SCC during the early 1970s, but the control of total hydrogen content was a concern. This concern remains in the potential use of newer polysiloxane technology, because coating suppliers do not consider hydrogen control to be a major design issue. Consequently, for future development, alternative coatings will be chosen based on their compatibility with existing fuel manufacturing processes and their ability to control the total hydrogen content in fuel sheath substrates. Although these factors are not explicitly examined in this work, they will be examined in future work.

¹ Cameco Fuel Manufacturing

² General Electric Hitachi - Canada

Despite these concerns, the numerous advantages afforded by polysiloxane technology give it tremendous potential as an alternative coating for protecting fuel sheaths against SCC. Polysiloxane technology has developed rapidly over the last two decades, and represents a new class of coating that has desirable characteristics and advantages over the older siloxane coatings. In particular, polysiloxanes have enhanced resiliency to radiation, high temperatures and combustion, and corrosive and oxidative environments. In addition, compared with the standard carbon-based CANLUB coating, polysiloxane coatings offer cost effectiveness, lower VOC content, low temperature cure capability, and improved methodology for their application.

Most significantly, polysiloxane coatings are inorganic polymers that are chemically stronger than organic CANLUB coatings. For instance, the resilience of polysiloxane stems from the Si-O building blocks (445 kJ·mol⁻¹), which are much stronger than the C-C blocks (358 kJ·mol⁻¹) in organic coatings. Silicon may be bonded to 2, 3, or 4 oxygen (O) atoms in the repeating backbone of the various polysiloxanes, rendering the 50-100% oxidized silicone immune to oxidative degradation, which is otherwise common among all organic coating substrates with carbon-only linkages. In addition, the highly polarized Si-O linkage protects any organic substituent (i.e., R = methyl, ethyl, phenyl) that is present in the backbone configuration as Si-R and/or Si-O-R [4].

2. Distinguishing Features of Candidate Coatings

This work examines the standard DAG154N (Deflocculated Acheson Graphite-154) coating and three commercial polysiloxane coatings (Table 1). Where possible, this section highlights the principal distinguishing features of these coatings. The DAG154N coating is a high quality, graphite-based coating designed to prevent deterioration in metals caused by oxidation or chemical action, with enhanced protection from the effects of thermal fatigue.

Coating	<u>Manufacturer</u>					
DAG154N	Henkel International / Acheson Colloids					
Pyromark	Tempil Inc. (Now LA-CO Industries Inc.)					
PSX 700	PPG Protective and Marine Coatings					
Wearlon 2020.98	Wearlon Industrial Coating Systems					

Table 1: Coatings and their manufacturers.

Pyromark is a single-component, silicone-based coating that protects metal surfaces exposed to high temperatures. It cures at room temperature (1 hour), provides long-lasting protection against oxidation and corrosion, and has excellent coverage characteristics with no blistering, chipping, cracking, or peeling at rated temperatures. Pyromark is applied by dip or brush application.

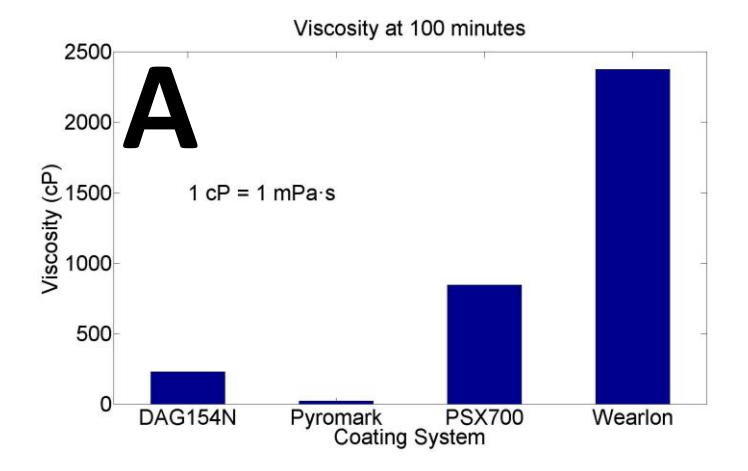
PSX 700 is an engineered high-gloss epoxy-siloxane coating. Its two components are hydrophobic silicone, and an epoxy that enables adhesion. With high durability and non-stick properties, it is highly resistant to abrasion. This solvent-based coating has ultra-low VOC and cures at room temperature (< 6 hours). PSX 700 is applied by spray, brush or roll.

In the Wearlon 2020.98 silicone topcoat, silicone molecules are chemically grafted throughout an epoxy matrix. Similar to the PSX 700, the water-based two-component Wearlon system is abrasion resistant, cures at room temperature, and has lubricity and non-stick properties. Again, silicone is the non-stick, hydrophobic component that provides lubrication, and the epoxy is a component that provides hardness (by reinforcing the brittle silicone) and enables adhesion.

3. Coating Characterization

3.1 Viscosity

The aforementioned coatings have been characterized based on fluid viscosity and thermal stability. The fluid viscosity was measured at given shear rates as a function of time (up to 120 minutes) using a Brookfield Viscometer (Model RVDV I+). During operation, a spindle immersed in a fluid is driven through a calibrated spring. Next, the viscous drag of the fluid against the spindle is measured by the spring deflection. Finally, the rotational speed of the spindle is measured with a rotary transducer and, depending on the shape and size of the spindle, the viscosity is determined and displayed in centipoise (cP). As shown in Figure 1A, the coating viscosities varied widely from 20 cP (Pyromark) to 2377 cP (Wearlon). These coatings were used as received without any attempt to lower the viscosity, because their chemical compositions were not available.



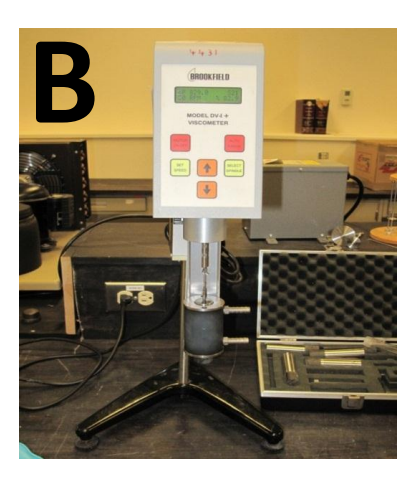


Figure 1: Coating viscosities (A) were recorded using a Brookfield viscometer (B) for ~ 2 hours at room temperature.

3.2 Thermogravimetric analysis (TGA)

The thermal stabilities of candidate coatings were evaluated using a Q50 thermogravimetric analyzer (TA Instruments), wherein the mass loss vs. temperature (up to 800°C at a ramp rate of 5°C min⁻¹) was measured in a nitrogen atmosphere. For a given temperature range, a sample is considered thermally stable when there is little to no slope in the TGA trace. Mass loss generally occurs at certain temperatures, which induce decomposition of specific components of the

coating samples. For instance, the TGA results from the four coatings (Figure 2) show that solvent evaporation occurred at approximately 150-200°C, and the additional decomposition of binders (larger negative slope) occurred above 300°C. Since it is most important to preserve the binders, which impart adhesion and strongly influence durability, flexibility, and toughness, the coatings were cured at a maximum temperature of 300°C.

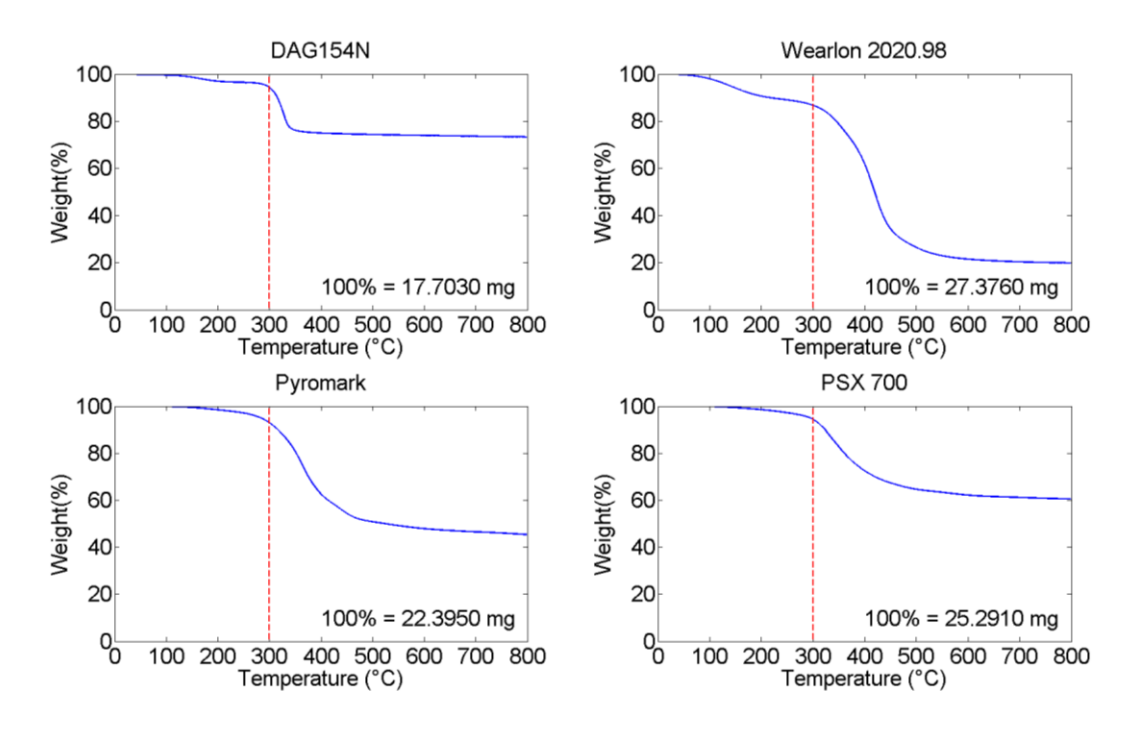


Figure 2: Change in mass as a function of temperature as measured by TGA.

4. Preparation of Zircaloy-4 Sheath Samples

A Buehler Isomet 1000 precision saw containing a 151-mm-diameter diamond blade was used for low-deformation cutting of Zircaloy-4 sheath samples (15.00 \pm 0.05 mm). These samples were sequentially polished using 220, 400, 600, and 800 grit silicon carbide paper, and then sonicated in ethanol for 20 minutes to eliminate metal shavings and dust.

The four coatings listed in Table 1 coated four sheath samples each (16 samples in total). From each four-sample set, two samples were coated fully and two samples were half-coated in the vertical direction. The samples were dipped in coating solutions for approximately 10 seconds, followed by four minutes of air-drying. This coating process was repeated three times. To expedite off-gassing, the coated samples were placed in a vacuum oven at 40°C (at 66 Torr) for six hours.

In preparation for curing, the coated samples were placed in a Pyrex tray and loaded into a programmable oven (MTI Corporation OTF-1200x) equipped with an Alcatel vacuum pump. The heating protocol – a 30-minute ramp to 300°C, a 1-hour hold at 300°C, and a 40-minute cool down to room temperature – was initiated when the pressure fell below 30 mTorr.

5. Elemental and Physical Characterization of Cured Coatings

After the sample preparations were completed, the cured coatings were characterized based on structural appearance, thickness, and elemental composition. A scanning electron microscope (Philips VP-30XL) coupled with energy dispersive X-ray spectrometry (EDX Apollo Detector and Genesis software) provided high magnification imaging, rapid non-destructive compositional analysis, and robust computer automation for evaluating the size, shape and elemental composition of all cured coatings. Cross-sectional scanning electron microscope (SEM) images of all four coatings on the Zircaloy-4 sheath are shown in Figure 3.

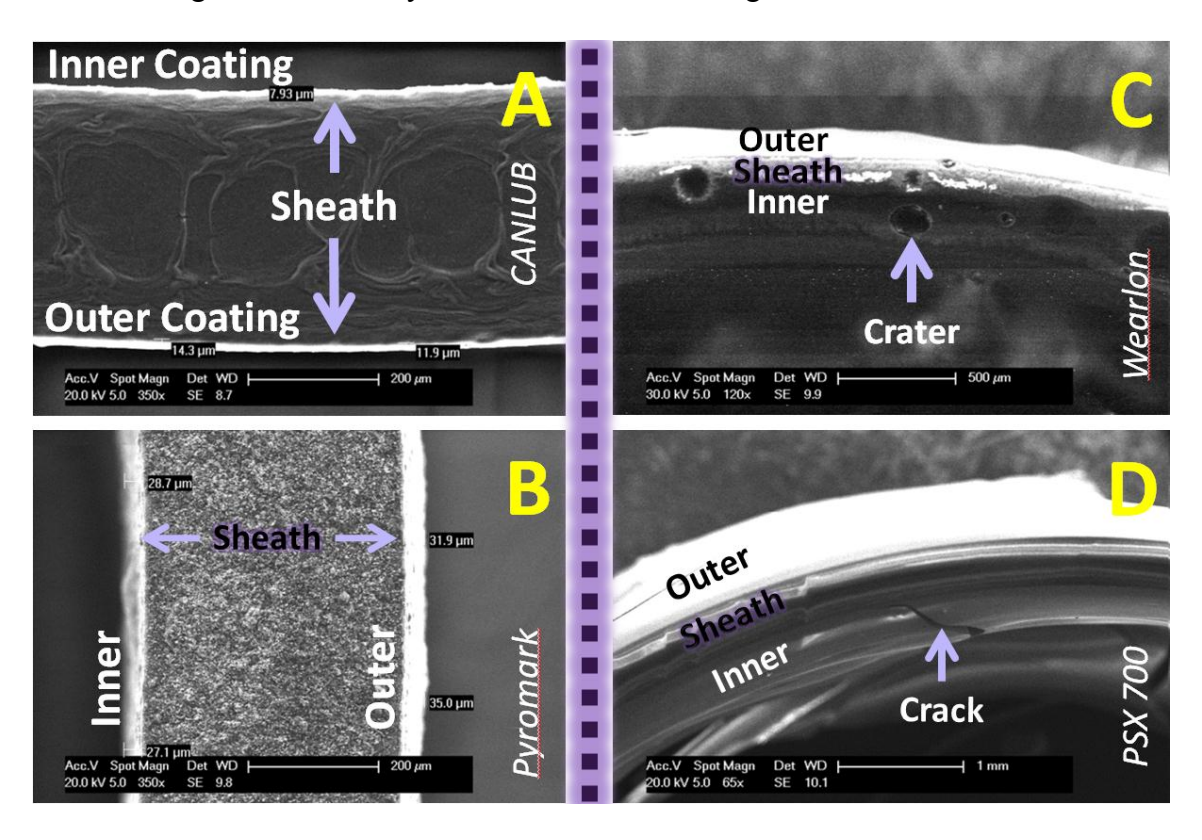


Figure 3: Low viscosity coatings (CANLUB (A) and Pyromark (B)) were uniformly coated, whereas the high viscosity coatings (Wearlon 2020.98 (C) and PSX 700 (D)) did not coat uniformly, and were susceptible to cracking and/or cratering.

The CANLUB coating is created via thermal decomposition of DAG154N components [3]. Consequently, we hereafter refer to the CANLUB coating rather than raw DAG154N. Compared with the CANLUB coating, the siloxane-based Pyromark coating has lower viscosity, comparably uniform coverage (Figures 3 and 4), and increased thickness (i.e., 30 µm vs. 10 µm). Conversely, the Wearlon 2020.98 and PSX 700 coatings exhibited much higher viscosities and thicknesses, but did not coat uniformly and suffered from cracking and/or cratering (Figures 3 and 4). The influence of curing condition was revealed in a second experiment, where coatings were cured in a nitrogen atmosphere, rather than in vacuum, to create a more inert environment. Figure 5 shows that coatings cured in nitrogen and in vacuum appeared structurally similar.



Figure 4: Uncoated Zircaloy-4 sheath sample, along with coated Zircaloy-4 sheath samples (after the coatings were baked). Half-coated samples facilitate the elemental analysis of uncoated and coated sections.



Figure 5: A second experiment was completed in a nitrogen atmosphere rather than in vacuum. Coatings cured in nitrogen and in vacuum appear structurally similar.

Unlike the Pyromark coating, the high-viscosity coatings are two-component systems, which are more susceptible to time-dependent processes. For instance, their already-high viscosities were observed to increase rapidly with time during individual viscosity measurements (not shown). For example, the Wearlon coating viscosity increased from 1642 cP to 2377 cP over 100 minutes. Furthermore, routine physical inspection of the post-baked high-viscosity coatings demonstrated their weak adherence to the Zircaloy-4, as they readily peeled from the sheath while enduring small shearing forces. By comparison, the adherence of the Pyromark coating to the Zircaloy-4 sheath was much stronger. Moreover, we discovered that high-viscosity coatings required a significantly longer room-temperature curing time (5 days vs. 1 day for Pyromark) before curing at 300°C could be initiated. When the high-viscosity coatings were cured for only one day at room-temperature, they yield significantly more cracking and/or cratering compared to those presented in Figure 4 (5-day room temperature cure).

Energy dispersive X-ray spectrometry was used for a preliminary non-destructive compositional analysis of all four coatings (Figure 6). As expected, the uncoated Zircaloy-4 sheath (Figure 6A) contains zirconium and the CANLUB-coated sheath (Figure 6B) contains carbon (graphite) and zirconium (from the sheath exposed during EDX testing). The Pyromark (Figure 6C), Wearlon 2020.98 (Figure 6D), and PSX 700 (Figure 6E) coatings contained silicon, oxygen, and carbon, with the PSX 700 coating also having iron and the Pyromark coating having iron and manganese. The high concentrations of silicon, oxygen, and carbon form the balance of the commercial siloxane-based coatings, where the carbon likely represents the adhesive epoxy. Additional elements inherently available in these coatings (e.g., iron and manganese) may provide chemical advantages. In particular, impurities such as sodium, aluminum, iron and silicon may be iodine scavengers [5,6].

Since the Pyromark coating compares favourably with the CANLUB coating across several key parameters, a more detailed elemental analysis on the Pyromark and CANLUB coatings was conducted using a PerkinElmer ELAN DRC II inductively-coupled plasma mass spectrometer (Table 2). The results confirm that Pyromark contains larger concentrations of potential iodine-scavenging elements (e.g., sodium, aluminum, iron and silicon), as well as a relative abundance of silicon that will likely enhance chemical strength (recall the strong Si-O).

6. Classic C-Ring Experimentation

Since the Pyromark coating has favourable physical, elemental, and chemical attributes, its performance as a protective coating was tested by subjecting four Pyromark-coated and four uncoated Zircaloy-4 C-rings to a five-day thermo-mechanical stress treatment in the presence of iodine [7,8]. Therefore, this section outlines the procedures for establishing a hot, stressful, and corrosive environment, and discusses the mitigation performance of the Pyromark coating against thermo-mechanical stress based on subsequent deflection measurements of the coated and uncoated rings as well as surface examination by scanning electron microscopy.

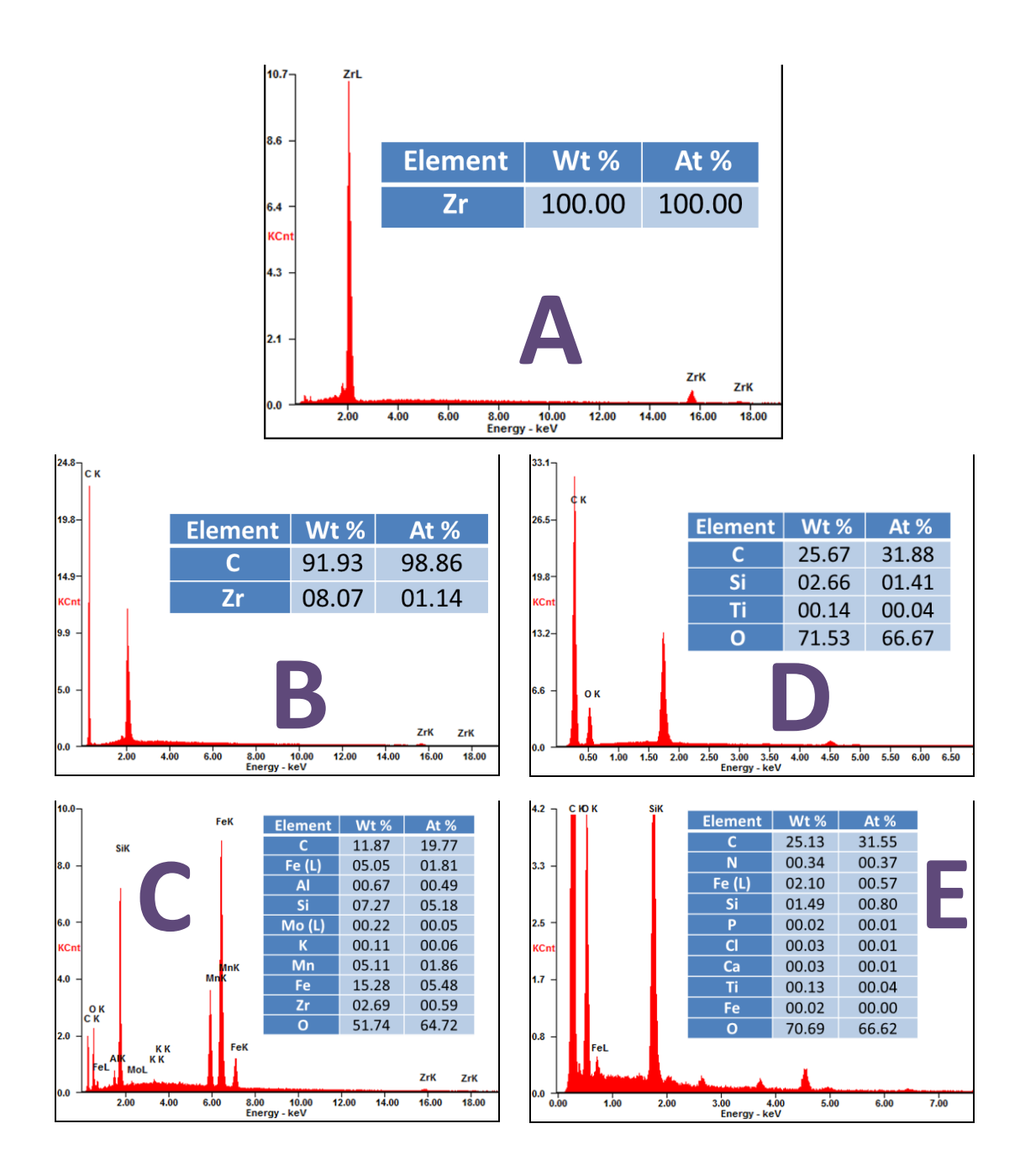


Figure 6: Elemental analysis by energy dispersive x-ray (EDX) spectrometry. (A) is the uncoated Zircaloy-4 sheath, and (B-E) are the CANLUB, Pyromark, Wearlon 2020.98, and PSX 700 coatings, respectively.

Table 2: Inductively-coupled plasma mass spectrometry (ICP-MS) analysis of the CANLUB and Pyromark coatings.

Element	Symbol	Unit	DAG-154	PyroMARK	Blank	Element	Symbol	Unit	DAG-154	PyroMARK	Blank	Element	Symbol	Unit	DAG-154	PyroMARK	Blank
Lithium	Li	ng/g	225	38,300	107	Selenium	Se	ng/g	67	0.0	775	Samarium	Sm	ng/g	55	640	0.0
Beryllium	Be	ng/g	3.0	92	0.0	Bromine	Br	ng/g	2,300	18,000	381	Europium	Eu	ng/g	6.0	190	0.3
Boron	В	ng/g	9,440	5,800	270	Rubidium	Rb	ng/g	12	2,000	2.6	Gadolinium	Gd	ng/g	190	710	0.0
Sodium	Na	ng/g	327,000	1,200,000	38,000	Strontium	Sr	ng/g	740	20,000	53	Terbium	Tb	ng/g	87	130	76
Magnesium	Mg	ng/g	7,370	840,000	2,300	Yttrium	Υ	ng/g	670	2,600	140	Dysprosium	Dy	ng/g	54	550	0.0
Aluminium	Al	ng/g	14,800	3,660,000	740	Zirconium	Zr	ng/g	2,000	4,900	4.1	Holmium	Но	ng/g	550	370	500
Silicon	Si	ng/g	24,800	263,000	0.0	Niobium	Nb	ng/g	88	2,100	0.4	Erbium	Er	ng/g	36	260	0.0
Phosphorous	P	ng/g	18,000	91,000	20,000	Molybdenum	Mo	ng/g	12,000	38,000	2.5	Thulium	Tm	ng/g	2.3	35	0.0
Chloride	Cl	ng/g	433,000	0.0	70,000	Ruthenium	Ru	ng/g	0.0	1.9	0.0	Ytterbium	Yb	ng/g	10	250	0.4
Potassium	K	ng/g	4,800	656,000	2,200	Rhenium	Rh	ng/g	650	0.0	720	Lutetium	Lu	ng/g	10	37	
Calcium	Ca	ng/g	100,000	0.0	9,900	Palladium	Pd	ng/g	2.0	61	0.0	Hafnium	Hf	ng/g	43	120	33
Scandium	Sc	ng/g	400	1,080	380	Silver	Ag	ng/g	10	190	0.7	Tantalum	Ta	ng/g	13	15	11 26
Titanium	Ti	ng/g	18,000	310,000	104	Cadmium	Cd	ng/g	40	610	0.0	Tungsten	w	ng/g	82	2,800	
Vanadium	V	ng/g	1,900	27,000	4.8	Indium	In	ng/g	95	19	123	Rhenium	Re	ng/g	0.1	3.0	0.0
Chromium	Cr	ng/g	2,800	150,000	69	Tin	Sn	ng/g	2,700	24,000	11	Osmium	Os	ng/g	0.0	0.4	0.0
Manganese	Mn	ng/g	5,300	ND*	260	Antimony	Sb	ng/g	31	458	10	Iridium	Ir	ng/g	0.7	1.2	0.0
Iron	Fe	ng/g	1,040,000	120,000,000	29,000	Tellurium	Te	ng/g	0.0	110	0.0	Platinum	Pt	ng/g	0.2	4.0	
Cobalt	Co	ng/g	92	55,500	1.8	lodine	I	ng/g	290	110	5.5	Gold	Au	ng/g	0.0	0.7	0.0
Nickel	Ni	ng/g	2,400	96,000	75	Cesium	Cs	ng/g	3.0	165	0.1	Mercury	Hg	ng/g	315	102	0.0
Copper	Cu	ng/g	1,500	264,000	71	Barium	Ba	ng/g	2,100	200,000	22	Tantalum	TI	ng/g	0.0	39	
Zinc	Zn	ng/g	1,100	123,000	155	Lanthanum	La	ng/g	770	4,100	0.0	Lead	Pb	ng/g	220	16,700	
Gallium	Ga	ng/g	270	4,100	243	Cerium	Ce	ng/g	970	11,000	0.4	Bismuth	Bi	ng/g	50	87	
Germanium	Ge	ng/g	28	160	0.0	Praseodymium	Pr	ng/g	96	820	0.1	Thorium	Th	ng/g	180	590	19
Arsenic	As	ng/g	77	11,500	2.7	Neodymium	Nd	ng/g	320	3,100	0.0	Uranium	U	ng/g	50	205	4.7

6.1 Establishing a hot, stressful, and corrosive environment for the C-rings

C-rings were cut (width = 5.00 ± 0.05 mm), fully-coated (when applicable), and cured using the procedures listed in Section 4. In addition, their narrow openings (2.30 ± 0.05 mm) were slotted using an Isomet saw. Experiments were conducted in a 250 mm long, medium-walled glass tube (25.4 mm O.D.) housing an unanchored, thin-walled glass vial containing iodine and an assembled mechanical stressing apparatus.

The glass vial was loaded with crystalline iodine $(1.800 \pm 0.001~g)$ and weighed while attached to a vacuum system. A virtually oxygen-free environment filled the vial after three freeze-pump-thaw cycles, and trace argon was subsequently introduced before the vial was sealed. The vial was sealed with a fragile gooseneck boundary to facilitate its eventual breakage and subsequent release of iodine into the glass tube. Both the sealed glass vial and the C-rings, stretched from 2.3- to 9-mm using a single-piece wedge (Figure 7), were placed into the glass tube, which was then attached to a vacuum line equipped with an Alcatel rotary pump and a Varian Turbo – V70D Macro Torr turbo molecular pump. After the desired vacuum level of 26 μ Torr or better was achieved, the glass assembly was heat-sealed.

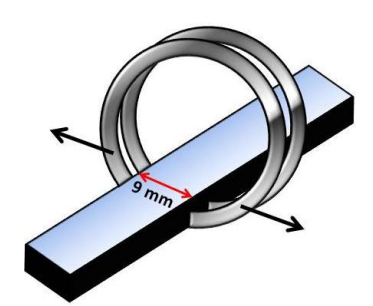


Figure 7: The Zircaloy-4 rectangular wedge exerts mechanical stress and stretches the coated Zircaloy-4 C-rings by increasing the slotted opening from 2.3 mm to 9 mm.

Within the heat-sealed glass assembly, the unanchored glass vial was brought into free-fall (by tilting the glass tube) and its subsequent collision with a tube boundary broke the vial and released iodine inside the glass tube. An operational temperature typically experienced by CANDU® fuel sheaths was established by placing the glass tube into a programmable oven (MTI Corporation OTF-1200x). After heating the stressed and iodine-exposed C-rings to 300°C for 5 days, the C-rings were extricated from the glass tube and subsequently released from the rectangular wedge in preparation for deflection measurements.

6.2 Deflection measurements

An apparatus was assembled to allow computer-aided deflection measurements [8] of the post-stressed C-ring samples (Figure 8). The rings were individually mounted on the apparatus and subjected to fixed weight-loads of 50 g and 100 g in succession, and the resulting deflections were measured using an Omega LD400 series displacement transducer (Table 3). Deflections of an as-fabricated C-ring were also measured for reference. After each deflection test, the unloaded slot opening (S) was re-measured to verify that weight-loads induced mainly elastic deformation.



Figure 8: Apparatus for deflection testing

Table 3: Slot openings (S), and their resulting deflections (Δx) when subjected to 50 and 100 g weight-loads. All values are in mm. The measurement errors for S and Δx are \pm 0.05 mm (Vernier caliper) and \pm 0.02 mm (variations over a 30 s loading time), respectively.

Untreated C-ring			Post-treated C-rings							
	Uniteated	C-ring		Coated (w/ Py	romark)	Uncoated				
S	$\Delta x (50 \text{ g})$	$\Delta x (100 \text{ g})$	S	$\Delta x (50 \text{ g})$	$\Delta x (100 \text{ g})$	S	$\Delta x (50 \text{ g})$	$\Delta x (100 \text{ g})$		
2.30	0.40	0.83	7.30	0.53	1.09	8.34	0.67	1.33		
			7.53	0.51	1.24	8.41	0.60	1.32		
			7.54	0.52	1.19	8.26	0.76	1.37		
			7.24	0.58	1.17	8.29	0.68	1.27		

During the five-day stress treatment, the rectangular wedge strained the slot opening from 2.3- to 9-mm. As this strain was maintained at constant temperature, the Zircaloy-4 experienced *stress relaxation* whereby the stress (σ) decreases exponentially with time (t) according to $\sigma/\sigma_0 = De^{-Kt}$, where σ_0 is initial applied stress, D is the unrelaxed stress ratio after an initial rapid stress drop, and K is a temperature-dependent relaxation rate constant [9]. During stress relaxation, the metal irreversibly changes its shape, which prevents the Pyromark-coated and uncoated Zircaloy-4 rings from fully rebounding to their original slot opening (2.30 \pm 0.05 mm) once the wedge is released.

Stress relaxation was less evident in the coated rings than in the uncoated rings. In other words, the coated rings were better able to rebound toward their original slot opening. This is likely because the Pyromark-coating absorbed a portion of the iodine, which helped to preserve some ductility in the Zircaloy-4 material. After releasing the rings from the wedge at room temperature, the slot openings of the coated and uncoated rings recovered from 9-mm to average values of 7.4 ± 0.2 mm and 8.33 ± 0.07 mm, respectively.

Post-stressed rings that permanently deform to wider equilibrium openings also surrendered increased deflections under a given weight-load. For example, at 50 g, the as-fabricated ring surrendered the lowest deflection ($\Delta x = 0.40 \pm 0.02$ mm) compared to the deflections of coated and uncoated rings enduring increasing levels of stress relaxation ($\Delta x = 0.54 \pm 0.03$ mm and 0.68 \pm 0.06 mm, respectively).

Finally, the load application produced a linear displacement response from 50 to 100 g in the as-fabricated ring and the post-stressed rings. Within experimental error, doubling the weight-load also doubled the induced deflection. This is clear when comparing the average deflections of the as-fabricated ring and the post-stressed (coated and uncoated) rings at 50 g ($\Delta x = 0.40 \pm 0.02$ mm, 0.54 ± 0.03 mm and 0.68 ± 0.06 mm, respectively) with the corresponding average deflections at 100 g ($\Delta x = 0.83 \pm 0.02$ mm, 1.17 ± 0.06 mm, and 1.32 ± 0.04 mm, respectively). In general, the deflection measurements show that the Pyromark coating limited stress relaxation and prevented excessive weakening of Zircaloy-4 C-rings strained in an iodine environment.

6.3 Surface examination by scanning electron microscopy

After a three-day thermo-mechanical stress treatment in the presence of iodine, Pyromark-coated and uncoated Zircaloy-4 C-ring surfaces were examined by scanning electron microscopy (SEM), and found to be clearly distinct (Figures 9A and 9B, respectively). After the Pyromark coating was removed (Figure 9A), SEM revealed a smooth surface morphology resulting from protection afforded by the coating. When an uncoated ring experiences the same stress treatment, its surface clearly indicates the initiation of surface attack (Figure 9B). Similar morphologies of the Pyromark-protected surface and an as-fabricated surface (Figure 9C) further suggest that the Pyromark coating protected the Zircaloy-4 C-ring surface.

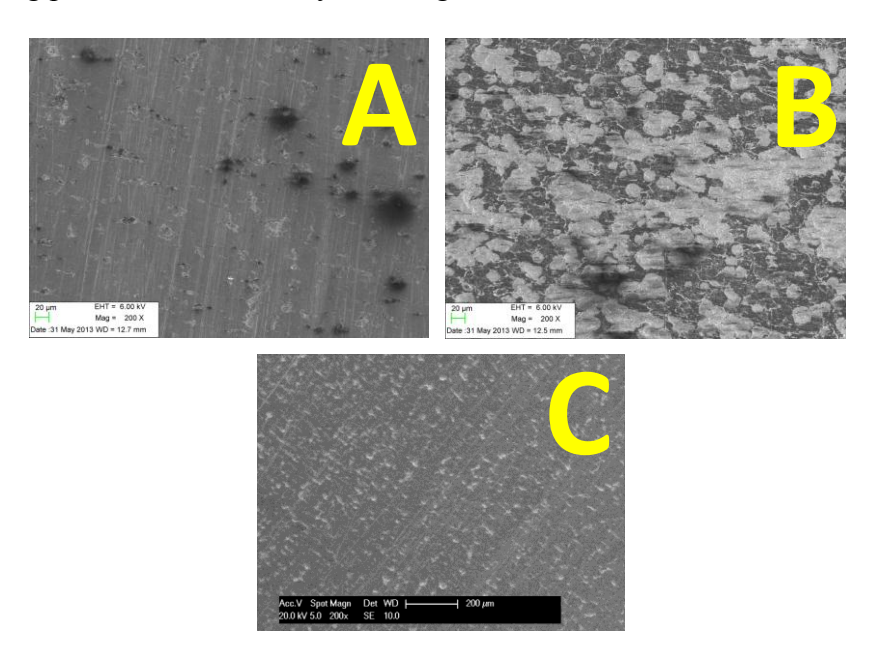


Figure 9: SEM images of post-coated (A) and uncoated (B) Zircaloy-4 surfaces after a three-day thermo-mechanical stress treatment. The Pyromark coating effectively protected the Zircaloy-4 surface (A) from the surface attack (white blotches) experienced by an uncoated surface (B). An as-fabricated Zircaloy-4 surface (C) compares favourably to the post-coated surface (A).

7. Summary and Future Work

DAG154N/CANLUB and three commercial polysiloxane coatings were characterized based on viscosity, thermal stability, structural appearance, thickness, and elemental composition. Coatings were cured at 300°C after the TGA showed that decomposition of binders occurred consistently above 300°C for all coatings. No major structural differences were observed between coatings cured in a nitrogen or vacuum environment.

The low-viscosity coatings adhered to the Zircaloy-4 smoothly and uniformly, while the high-viscosity coatings adhered non-uniformly and exhibited cracks and/or craters. Since the low-viscosity coatings exhibit similar characteristics, it can be suggested that Pyromark can be applied using existing manufacturing processes. In addition, EDX and ICP-MS analysis revealed greater concentrations of potential iodine scavengers (e.g., sodium, aluminum, iron and silicon) in the Pyromark coating, which may provide enhanced chemical protection against iodine.

After a three- or five-day thermo-mechanical stress treatment in the presence of iodine, the Pyromark coating successfully prevented degradation of the Zircaloy-4 surface due to corrosion. This apparent protection limited the permanent deformation of Zircaloy-4, and prevented excessive weakening as evidenced by lower load-induced deflections compared with those surrendered in uncoated C-rings. Although these results are encouraging, they are also limited so more systematic tests are being planned. Upcoming experiments will also address the potential advantages of the Pyromark coating offered by its elemental distribution. In particular, future work will investigate the performance of additional polysiloxane coatings, as well as the potential benefits associated with doping the existing DAG154N coating with Na₂O (<1% w), which is one of the impurities found in CANLUB by Lewis *et al.* [5]. The Na impurity is expected to be present as an oxide or carbonate after pyrolysis of CANLUB. In either case, Na is expected to gather iodine by forming the compound, NaI. Finally, we will assess the nature of the observed surface attack in Zircaloy-4 samples.

8. References

- [1] M.R. Floyd, J. Novak, and P.T. Truant, "Fission-gas release in fuel performing to extended burnups in Ontario Hydro nuclear generating stations", AECL-10636, 1992.
- [2] P.K. Chan, K. Franklin, D.A. Guzonas, J. Halliday, and K.J.W. Kaddatz, "The active "ingredient" in CANLUB", 4th Annual Conference on CANDU Fuel, Pembroke, Ontario, October, 1995.
- [3] M.R. Floyd, "Extended burnup CANDU fuel performance", 7th International CANDU Fuel Conference Proceedings, Kingston, Ontario, Canada, September 23-27, 2001.
- [4] W.A. Finzel and H.L. Vincent, "Silicones in coatings", In: Federation Series on Coatings, Federation of Societies for Coatings Technologies, Blue Bell, PA, 9, 1996.
- [5] B.J. Lewis, W.T. Thompson, M.R. Kleczek, K. Shaheen, M. Juhas, and F.C. Iglesias, "Modelling of iodine-induced stress corrosion cracking in CANDU fuel", Journal of Nuclear Materials, Vol. 408, No. 3, pp. 209-223, 2011.

12th International Conference on CANDU Fuel

Holiday-Inn Waterfront Hotel Kingston, Ontario, Canada, 2013 September 15-18

- [6] M.R. Kleczek, "Thermodynamic and kinetic modelling of iodine induced stress corrosion cracking in nuclear fuel sheathing", M.A.Sc. Thesis, Royal Military College of Canada, Kingston, Ontario, 2010.
- [7] J.C. Wood, "Factors affecting stress corrosion cracking on Zircaloy in iodine vapor", Journal of Nuclear Materials, Vol. 45, pp. 105-122, 1972/1973.
- [8] A.D. Quastel, E.C. Corcoran, and B.J. Lewis, "The effect of oxidized UO₂ on iodine-induced stress corrosion cracking of fuel sheathing" <u>12th International CANDU Fuel Conference</u>, Kingston, Ontario, September 15-18, 2013.
- [9] A.R. Causey, "In-reactor creep of zircaloy-2, zircaloy-4 and Zr-1.15 wt % Cr-0.1 wt % Fe at 568 K derived from their stress-relaxation behaviour", Journal of Nuclear Materials, Vol. 54, No. 1, pp. 64-72, 1974.

9. Acknowledgements

The authors acknowledge the Natural Sciences and Engineering Research Council of Canada, and Cameco Fuel Manufacturing Incorporated for financial support. Many thanks go to Jennifer Snelgrove for performing the SEM and EDX experiments.